Environmental Science and Pollution Research (2022) 29:66422–66437
https://doi.org/10.1007/s11356-022-20520-7

RESEARCH ARTICLE

Copaiba oil and vegetal tannin as functionalizing agents for açai nanofibril films: valorization of forest wastes from Amazonia

Mário Vanoli Scatolino[1,2] · Lina Bufalino[3] · Matheus Cordazzo Dias[4] · Lourival Marin Mendes[4] · Mateus Souza da Silva[4] · Gustavo Henrique Denzin Tonoli[4] · Tiago Marcolino de Souza[5] · Francisco Tarcisio Alves Junior[1,2]

Received: 22 December 2021 / Accepted: 25 April 2022 / Published online: 3 May 2022

Abstract

The applicability of cellulose nanofibrils (CNFs) has received attention due to their attractive properties. This study proposes the functionalization of açai CNFs with copaiba oil and vegetal tannins to produce films with potential for packaging. Bio-based films were evaluated by vapor permeability, colorimetry, and mechanical strength. CNFs were produced by mechanical fibrillation, from suspensions of bleached açai fibers and commercial eucalipytus pulp. Moreover, copaiba oil and vegetal tannin were added to the CNFs to produce films/nanopapers by casting from both suspensions with concentrations of 1% (based on CNF dry mass). The bulk densities of the eucalyptus CNF films were higher (1.126–1.171 g cm^{-3}) compared to the açai CNF ones. Films from eucalyptus and açai pulps containing copaiba oil and tannins presented higher *Tonset* and *Tmax*, respectively (312 and 370 °C). Films with açaí CNFs functionalized with copaiba oil and tannin showed the lowest permeability value (370 g day^{-1} m^{-2}). Films produced with eucalyptus pulp, and eucalyptus pulp functionalized with copaiba oil highlighted by superior mechanical strength, achieving 133.8 and 121.4 MPa, respectively. The evaluation of colorimetry showed a greater tendency to yellowing for açai films, especially those functionalized with vegetal tannins. Besides the low cost, functionalized vegetal-based nanomaterials could have attractive properties, with potential for application as some kind of packaging, for transporting basic products, such as breads, flours, or products with low moisture content, enabling efficient utilization of forest wastes.

Keywords Bio-based material · Fibrillated cellulose · Brazilian resources · Productive chain

Responsible Editor: Philippe Garrigues

✉ Mário Vanoli Scatolino
marioscatolino@gmail.com

Lina Bufalino
linabufalino@yahoo.com.br

Matheus Cordazzo Dias
matheus.cordasso@gmail.com

Lourival Marin Mendes
lourival@ufla.br

Mateus Souza da Silva
mateus.ss10@gmail.com

Gustavo Henrique Denzin Tonoli
gustavotonoli@ufla.br

Tiago Marcolino de Souza
tiago.souza@ueap.edu.br

Francisco Tarcisio Alves Junior
tarcisioalvesjr@yahoo.com.br

[1] Department of Production Engineering, State University of Amapá – UEAP, Macapá, AP, Brazil

[2] PROFNIT - Postgraduate Program on Intellectual Property and Technology Transfer for Innovation, Federal University of Amapá – UNIFAP, Macapá, AP, Brazil

[3] Department of Forest Sciences, Rural Federal University of Amazonia – UFRA, Belém, PA, Brazil

[4] Department of Forest Sciences, Federal University of Lavras – UFLA, Perimetral Av., POB 3037, Lavras, MG, Brazil

[5] Department of Chemical Engineering, State University of Amapá – UEAP, Macapá, AP, Brazil

Introduction

Technologies to produce nanostructured materials with resistance to microorganisms harmful to human health are growing fast. To achieve this yearning, the functionalization of raw materials with vegetal extracts has gained visibility in worldwide research. In Brazil, where Amazonia is located, a vast diversity of raw materials can be exploited following the precepts of sustainable management. Amazonia forest offers from varied wood species (Scatolino et al. 2017) to several non-woody forest products, such as oils, resins, tannins, and gums (Pena et al. 2021). In this context, an increased interest in natural oils and phenolic compounds with complex chemical compositions, such as copaiba resin oil and vegetal tannin, emerges from their great potential for developing phytoproducts to applications in pharmaceutical, cosmetic, sanitary, and food industries.

A possible alternative for using non-woody products like oils is their incorporation into films and nanostructured composites, especially those produced with plant nanofibrils. Cellulose nanofibrils (CNFs) show diameters in nanoscale, varying from 10 to 100 nm, being attained using a specialized microfibrillator (grinder), a mechanism consisting of forcing fibers through an opening between a rotating stone and a static one (Scatolino et al. 2018). One of the biggest problems with this method is the high power consumption. Guimarães et al. (2021) found power consumption of ~4.4×10^3 kWh/ton after 20 cycles of fibrillation for eucalyptus commercial pulp and pseudostem tree fiber. Similarly, Dias et al. (2019) obtained ~13×10^3 kWh/ton for power consumption when fibrillating commercial pinus pulp after 30 cycles through the grinder. Other fibrillation methods are also efficient for cell wall deconstruction, such as homogenization and microfluidization (Bian et al. 2018), besides chemical and enzymatic methods. Furthermore, nanotechnology has improved the performance of hydrophobic compounds, increasing the stability and solubility of molecules and decreasing cytotoxicity and undesired drug interactions (Amaral et al. 2009).

Vegetal fibers have been explored for the production of nanostructured films and nanocomposites, such as banana pseudostem tree fiber (Guimarães et al. 2021), pineapple (Abraham et al. 2011), jute (Fonseca et al. 2021), palm tree (Okahisa et al. 2018), cotton (Chen et al. 2014), sisal (Santana et al. 2017), bamboo (Guimarães Jr et al. 2018), oat straw (do Lago et al. 2020), cocoa shell (Souza et al. 2019), red cedar bark (Zhang et al. 2019), and others. In addition to the use of vegetal fibers from non-woody sources, natural additives such as copaiba oil and tannins do not require the species felling for extraction, keeping the trees in a constant state of production. Copaiba oil and tannins are usually extracted from non-vital parts of the plant, such as bark and leaves, or through small incisions in the trunk. Morelli et al. (2015) intensively researched copaiba oil as an antibacterial agent for bio-based active packaging. Debone et al. (2019) studied the effect of copaiba oleoresin and chitosan in the properties of films for application as dressings and skin burns. Furtado et al. (2021) revealed the association of babassu oil and copaiba oil resin in a nanosystem as a potential phytotherapic alternative for treatment and prophylaxis of benign prostatic hyperplasia.

Condensed tannins are the most abundantly extracted natural substances on Earth, with 200 thousand tons extracted each year (Pizzi 2008). Vegetal tannins are known to be responsible for several functions in CNF films. Missio André et al. (2018) produced tannin-added films aiming to develop a nontoxic packaging material for food and pharmaceutical products. Cano et al. (2021) used vegetal tannins applied to cellulose compounds with the intention to produce less water-soluble, mechanically stiffer, and less stretchable films. Additionally, Zhou et al. (2019) used tannins and nanocellulose to develop polymer structures with antioxidant properties.

The literature clearly shows the potential of copaiba oil to offer antibacterial and antifungal properties to film/nanopapers, as many researchers have been committed to study this function. However, there is a lack of clear scientific evidence about their role in the films' mechanical, colorimetric, and barrier properties, which is extremely important in packaging applications. Characterizations on suspensions, such as stability, and on functionalized films with oils and tannins, such as mechanical properties, appear as novelty, since these conditions are not widely found in literature. Suspension stability is important to be evaluated, as it provides information on how nanofibrils behave when functionalized with other components. The mechanical properties of functionalized films are also important to assess determined additives showing a feasible interaction, or not. This information serves to complete results found in other articles. Therefore, this study proposes the functionalization of açai CNFs with copaiba oil and vegetal tannins to produce films with potential for packaging applications.

Material and methods

Material obtainment

Açai wastes composed of seeds covered with fibers were collected in a commercial establishment called "batedeira," where fruits are commonly processed for pulp extraction. The fruits were obtained from plantations of *Euterpe oleracea* Mart., region of Paragominas, State of Pará, PA. Açai

fibers were hand-removed and subjected to analysis to determine the basic density, following adapted procedures described in NBR 11941 standard (ABNT 2003). The basic density of açai fibers was 0.322 g cm^{-3}, a value comparable to some light woods. A commercial bleached *eucalyptus* pulp, obtained from kraft chemical pulping process (yields of 50–60%), with high brightness index of 92% ISO and viscosity of 675 $cm^3.g^{-1}$, was supplied by Suzano Paper and Cellulose (Suzano - SP, Brazil). Copaiba oil (*Copaifera* sp.) presenting a density of 0.865 g cm^{-3} was hand extracted, filtered, and packaged in the Vale do Jamarí, RO region. The entire storage and distribution process is carried out in a family environment. The vegetal tannin was donated by TANAC S. A (Montenegro, RS, Brazil), which extracts it from *Acacia mearnsii* species.

Pre-treatments of the fibers and pulp

Alkaline pre-treatment of the açai fibers was performed following the procedures described in Yue et al. (2015), using 100 mL of a 5% (w/v) NaOH solution (Êxodo Científica Inc.; SP, Brazil; purity grade 99%) for each 5 g of dry fibers, for 2 h at 80 °C (water bath) and under mechanical stirring (1500 rpm). For each 5 g of the previously alkaline-treated fibers, bleaching was performed using 100 mL of a solution 1:1 (v/v) of H_2O_2 (Bianquímica; SP, Brazil; purity grade 35%) at 24% (v/v) and NaOH at 4% (w/v) for 2 h at 80 °C (water bath) and with mechanical stirring (1500 rpm). After filtration, to remove the excess water with reagents, fiber samples were continuously washed with water and acetic acid solution 20% (v:v) until neutral pH. Açai fibers did not pass by the same pulping process as eucalyptus pulp. The commercial pulp underwent alkaline pre-treatment in similar conditions to that carried out for açai fibers. The material loss after the commercial bleaching process is between 2.5 and 5.0%. The yield of alkaline and bleaching treatments of açai fibers was 81% and 76%, respectively.

Obtaining the CNFs and the films

The bleached açai fibers and the commercial eucalyptus pulp were dispersed separately in 4 L of water and stirred for 30 min (200 rpm), obtaining a suspension of 2% concentration (based on fibers' dry mass). The CNFs from each raw material were obtained using a Masuko Supermasscolloider mechanical fibrillator (grinder) at 1600 rpm (Fig. 1) and keeping an average consumed electrical current of around 3.5–4.4 A, following the methods suggested by Bufalino et al. (2015). The suspensions were fibrillated in cycles of 5 passages through the Supermasscolloider. This number of passages was enough to provide a gel appearance for both suspensions. For both raw materials, the first passage was proceeded with distance of 50 µm between the discs, and the following passages were made with distance adjusted to ~0 µm (minimum possible). The açai pulp took about 4 min per passage, whereas each passage of the eucalyptus commercial pulp took nearly 150 s. The power consumption was ~4.1×10^3 kWh/ton for the commercial pulp and ~7.7×10^3 kWh/ton for the açai raw material. To promote the compatibility between CNFs and copaiba oil, 1% of Tween

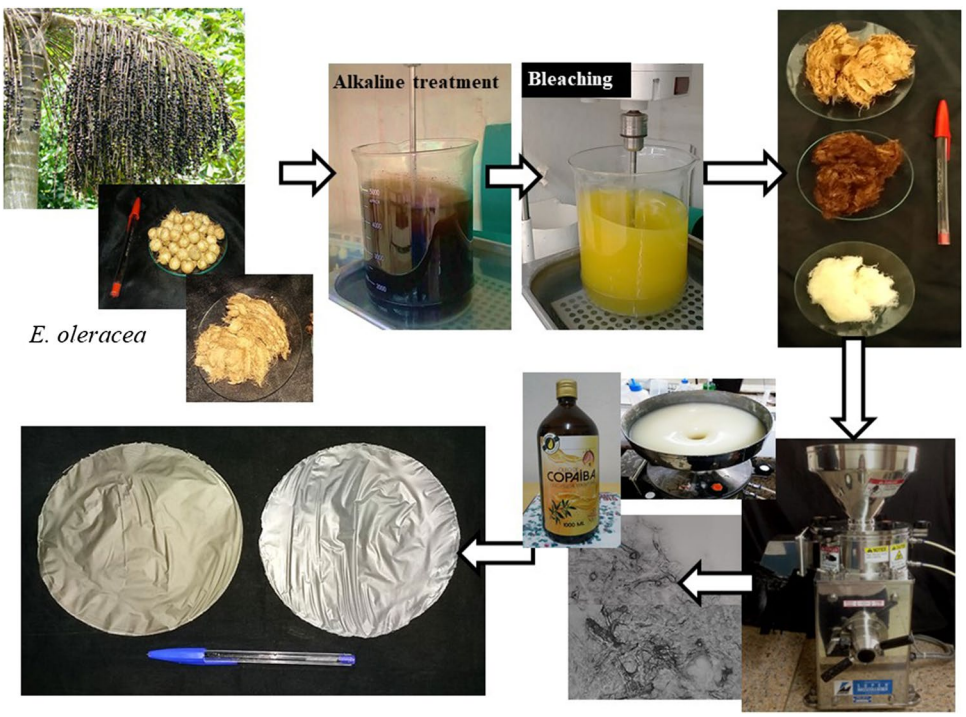

Fig. 1 Illustrative sequence of the pre-treatments, fibrillation, and CNF films production.

80 (Labsynth; SP, Brazil) was added (based on CNFs' dry mass). Tannin powder was manually mixed with the CNF suspension at a tannin-to-cellulose ratio of 1/5, as described in Missio André et al. (2018), and then stirred for 24 h to ensure complete dissolution. Aliquots of 60 mL of CNF suspension with a concentration of 1% (based on CNFs' dry mass), previously sonicated with an Eco-sonics sonicator (563 W of power), were poured on acrylic Petri dishes (15 cm diameter) for water evaporation in a conditioned room (20 ± 3 °C; RH ~65%). Four nanostructured film samples were produced from each treatment, totaling 24 flexible films (Table 1).

Chemical composition of the fibers

Determination of extractives and mineral/ash contents followed the TAPPI standard (2017) and TAPPI standard (2012b) standards, respectively. Contents of cellulose, hemicelluloses, and lignin of the natural and bleached fibers were obtained using samples after extractives removal. The insoluble lignin content was determined according to the procedures described in TAPPI standard (2002). The holocellulose content (based on extractives-free mass) was determined according to Browning (1963). Cellulose content was obtained following the methodology proposed by Kennedy et al. (1987). The weight difference between holocellulose and cellulose contents provides the hemicelluloses one. The average values of each component resulted from 4 replicates.

Stability of the suspensions

Stability of the suspension samples was conducted according to Guimarães Jr et al. (2015). The suspensions were diluted to 0.25 wt%, and aliquots of 15 mL were placed in test tubes for image acquisition. Images were acquired hourly for 8 h. Image J software (Schindelin et al., 2012) was used to estimate CNF decantation in the suspensions, and then stability was calculated according to Eq. 1.

$$S_t = \frac{D_h}{T_h} x\ 100 \quad (1)$$

where S_t is the suspension stability (%); D_h is the height of the dispersed suspension (cm); and T_h is the total liquid height inside the tubes (cm).

Water retention index

The water retention index (WRI) of the pulps was determined following the procedures described in Scandinavian test method SCAN – C 62:00 (2000), dispersing them in water at a fiber content of 0.5 wt% after boiling for 5 min. The water of suspensions was separated from the solid fraction using a Heraeus Megafuge 16R Centrifuge (Thermo Fisher Scientific, Waltham, MA, USA), with force of 3000 G for 15 min, and then the wet samples were weighed. After oven-drying at 110 °C for 5 h, the weight was measured again. The WRI was determined according to Eq. 2.

$$WRI = \frac{W_0 - W_1}{W_0} x\ 100 \quad (2)$$

where *WRI* is the water retention index (%); W_0 is the mass of the wet pulp (g); and W_1 is the mass of the oven-dried pulp (g).

Structure of the CNFs

The structure of the CNF suspensions was analyzed using a Tescan FEG Clara UHR scanning electron microscope with a voltage of 20 keV. Drops of nanocellulose suspensions were placed on double-sided carbon tape adhered to aluminum sample holders (stubs) and covered with gold before analysis. Micrographs were obtained from suspensions of both raw materials. The software *ImageJ*® was used to determine the samples' diameters and CNFs' details. The average CNFs' diameter was determined by 100 measurements proceeded in the SEM-FEG micrographs. The software provided the dimensions proportionally to the scale (known distance) in the scanning electron microscope.

Table 1 Experimental design of the project.

Raw material	Pre-treatment	Film	Total films produced
Açai fibers' pulp	Control	*A-CNFs*	4
	Copaiba oil (5% wt)	A_{CO}*-CNFs*	4
	Acacia tannin + copaiba oil (5% wt)	AT_{CO}*-CNFs*	4
Bleached eucalyptus pulp treated with NaOH	Control	*E-CNFs*	4
	Copaiba oil (5% wt)	E_{CO}*-CNFs*	4
	Acacia tannin + copaiba oil (5% wt)	ET_{CO}*-CNFs*	4

Bulk density and grammage of the films

A Mitutoyo micrometer was used to obtain the thickness and a digital caliper to measure the diameter. Samples were weighted at a precision of 0.1 mg, and grammage was expressed as mass (g) per area (m^2). The bulk density was calculated by dividing the films' mass by its volume. The results of bulk density and grammage were subjected to analysis of variance (ANOVA) ($p < 0.05$). The Scott-Knott test ($p < 0.05$) was performed in case of a significant difference between the averages.

Thermal degradation of the films

Samples containing around 4 mg were cut for thermogravimetric analysis (TGA). The film's thermal degradation was executed in a TGA Q500 (TA Instruments ®) thermal analyzer. Samples were heated at 10 °C/min from room temperature up to 600 °C, under a nitrogen atmosphere and using a gas flow of 50 mL/min. The initial degradation temperature (T*onset*) was obtained by the intersection of tangents to the constant mass region and the linear part of the curves after the deflection point, as described in Scatolino et al. (2018). Similarly, the percentage of residues was obtained by the final point of the curve. The temperature of maximum degradation (T*max*) was obtained through the peaks observed on the DrTGA curves.

Grease resistance of the films

The grease resistance test was proceeded according to TAPPI T559 standard (TAPPI standard 2012a), commonly known as the KIT test (Fig. 2). The procedures were based on the drip of reagents with various surface tension and viscosity or "aggressiveness" on the sample surface. Solutions were classified from 1 (less aggressive and composed only of castor oil) to 12 (more aggressive and composed of toluene and n-heptane). Five film samples of each composition were evaluated. A drop of oily solution was applied on the sample surface, being removed after 15 s of contact with the film. Each film composition was classified with the highest score (from 1 to 12) corresponding to the solution that did not cross the sample.

Water vapor transmission rate

The water vapor transmission rate (WVTR) of the films/nanopapers was carried out following the permeability cell methodology described in Guimarães Jr et al. (2015), which was based on ASTM E 96-00 (2000). This method determines the amount of water vapor that passes through a known sample area, induced by the vapor pressure difference between two specific points, one outside and the other inside the permeability cell. Samples with a diameter of 1.5 cm were sealed in a glass permeation cell containing silica gel (0% of relative humidity; with no water vapor pressure), placed inside a desiccator (containing NaOH solution) at 36 °C and with 90% of relative humidity (Fig. 3). The film/nanopaper was positioned in the glass bottle cap, forming a membrane between the exterior and interior of the permeability cell. The desiccator with the samples was placed inside a BOD (biochemical o*xygen demand), and* the permeability cell's mass was measured every 48 h for 10 consecutive

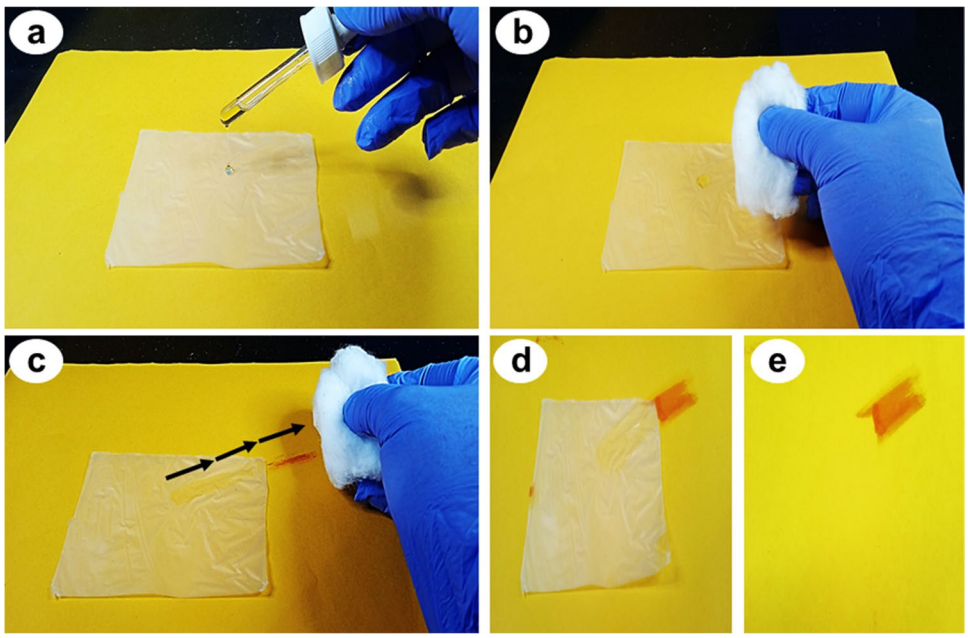

Fig. 2 Illustrative sequence of the grease resistance test; **a** a drop of oily solution is dripped on the film; **b** the drop is kept in contact for 15 s with the film; **c** a piece of cotton is passed over the region where the drop acts, by a movement that extends until the "solution trail" (black arrows) reaches the yellow paper positioned below the film; **d** and **e** the yellow paper below is analyzed for the traces of oily solution that possibly crossed the film.

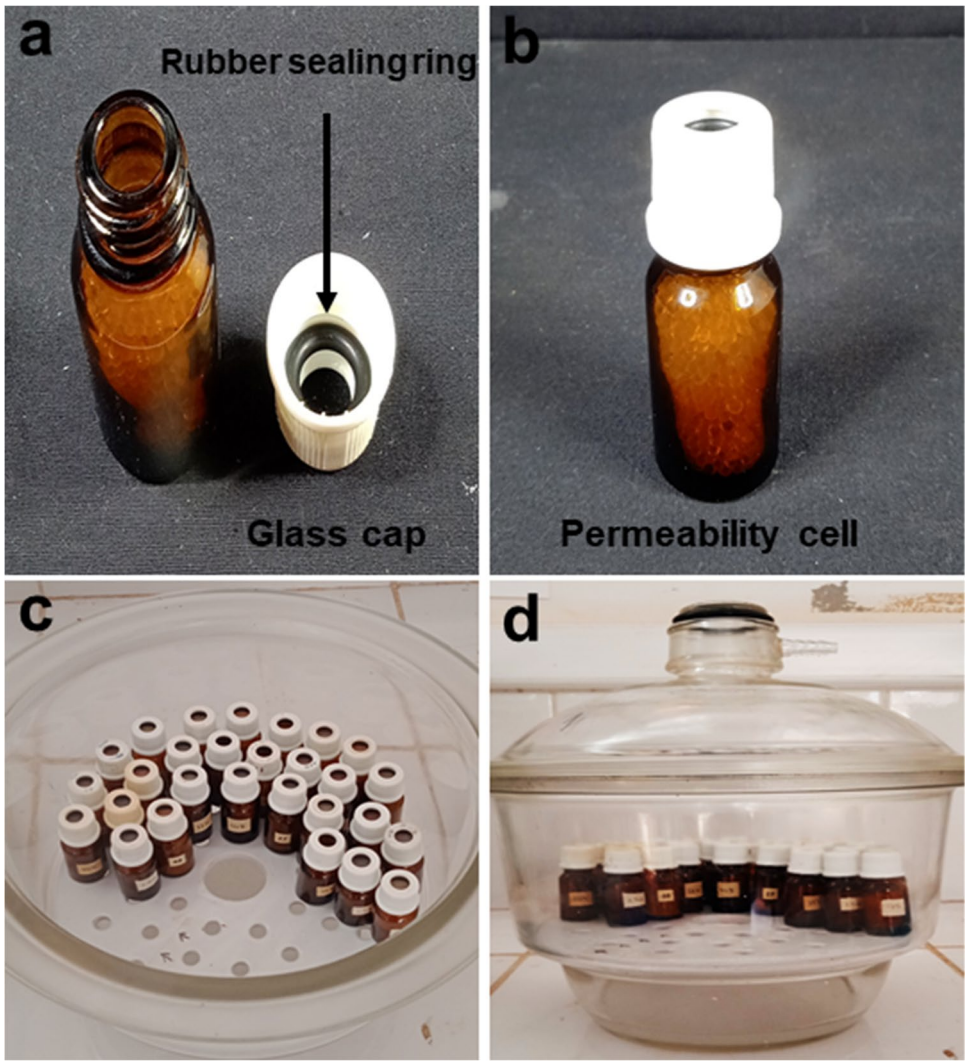

Fig. 3 Illustrative scheme of water vapor permeability test: **a** glass cap and rubber sealing ring; **b** permeability cell; **c** and **d** permeability cells inside the desiccator.

days. Four samples per treatment were evaluated. The values of WVTR (g $day^{-1}m^{-2}$) were calculated by Eq. (3).

$$WVTR = \frac{G}{dxA} \tag{3}$$

where *WVTR* is the water vapor transmission rate, *G/d* is the angular coefficient obtained by linear regression of the mass gain (g) versus conditioning time (days) graph, and *A* is the sample permeation area (m^2).

Mechanical properties of the films

Mechanical tests were performed according to ASTM D 882-18 (2018), using a texturometer (Stable Micro Systems, TATX2i, England) equipped with a load cell with capacity of 500 N. The tensile strength was evaluated from the average value of ten specimens (10 × 100 mm). Additionally, the graph with stress-strain curves was generated aiming to observe the mechanical behavior of the films. Before the test, the thickness of the samples was measured. The initial distance between the grips was 50 mm, and the test was conducted at speed of 5 mm/s.

Colorimetric properties of the films

The color of the films were determined with three replicates using a Minolta® CR-400 colorimeter (Tokyo, Japan) equipped with a 30-mm opening cell. The color and opacity in the reflectance mode of the samples were determined according to Eq. 4 (Paschoalick et al. 2003). In addition, *b* values were shown and analyzed.

$$\Delta E = \left[\Delta L^2 + \Delta a^2 + \Delta b^2\right]^{0.5} \tag{4}$$

where ΔE is the color index; ΔL is the difference in luminosity; Δa is the difference in color in the region from red to green; and Δb is the difference in color in the region from yellow to blue.

Results and discussion

Chemical composition of the fibers

The sequence of treatments performed on the açai fibers caused total extractives and partial insoluble lignin removal (Table 2). Extractives are colloidal substances containing triglycerides that are saponified during alkaline treatment, releasing free fatty acids and glycerol (Leiviskä et al. 2009). The presence of extractives in the bleached fibers and commercial pulp was not detected. Extractives are not chemically bonded to the plant cell wall structure; therefore, they are easily removed by simple treatments such as alkaline and cold and/or hot water.

Cellulose contents increased with the bleaching treatment, ranging from 34 to 56%. Commercial eucalyptus pulp treated with NaOH solution obtained a cellulose value of 76%. The cellulose contents of pulp from açai could be same or close that of eucalyptus pulp when the açai fibers were treated with more severe condition. Despite the known efficiency of alkaline and bleaching treatments, lignin was not wholly removed from the natural açai fibers. Total lignin (insoluble + soluble) was reduced from ~38% to ~19% for açai fibers, which is still a considerable amount after the sequence of treatments. High levels of lignin in the pulp can hinder the fibrillation process since this component provides rigidity to the cell wall and can offer greater resistance against shear and impact forces, interfering with energy consumption. As previously mentioned, the power consumption was ~4.1×10^3 kWh/ton for the commercial pulp and ~7.7×10^3 kWh/ton for the açai raw material, confirming the higher energy expenditure for the material richer in lignin. Similarly, treatments did not reduce hemicellulose content in the açai fibers. The low efficiency in removing non-cellulosic components may be related to the types of lignin and hemicelluloses present in the açai waste fiber. Depending on the component source, bonds may be more strongly connected with the cell wall, generating greater resistance to removal. The chemical composition of lignin varies from plant to plant, and even plants of the same family hold compositional differences in their tissues and layers. Additionally, the structural and physical characteristics of lignin are also influenced by the precursor species (Linan et al. 2021). Fibers with a high lignin content are excellent in quality and very flexible (Agrawal et al. 2000). Regarding hemicelluloses amount, Coutts and Warden (1992) state that its percentage can even increase after treatments depending on the specific type of fruit that originates the fibers and its growing conditions. Such changes are caused by reactions between fibers and the treatment solution.

Table 2 Chemical composition of açai fibers (*in natura* and bleached) and commercial eucalyptus pulp (after the alkaline treatment).

Component	Açai *in natura*	Açai bleached	*Eucalyptus*
Total extractives (%)	4 ± 0.25	-	-
Insoluble lignin (%)	36 ± 0.69	17 ± 3.65	0.14
Soluble lignin (%)	2 ± 0.11	2 ± 0.11	-
Ashes (%)	1.60 ± 0.19	0.35 ± 0.12	0.03
Holocellulose (%)	60 ± 2.02	81 ± 2.83	90
Cellulose (%)	34 ± 1.80	56 ± 0.17	76
Hemicelluloses (%)	26 ± 1.90	25 ± 0.16	14

The water retention index (WRI) values were 1.43, 1.09, and 1.04 for the *eucalyptus* commercial pulp, açai *in natura*, and bleached fibers, respectively. These results show that commercial eucalyptus pulp tends to absorb more water than açai fibers, probably due to lignin and extractives not completely removed with the treatments. These non-cellulosic components can provide a certain barrier against water absorption. In addition, the commercial eucalyptus pulp was composed practically of celluloses and hemicelluloses due to the pulping and bleaching treatments carried out in the industry, which implies more hydroxyl groups available for bonds with water. Alkaline and bleaching treatments are commonly used in the pulp and paper industries (Leiviskä and Rämö 2008).

Stability of the suspensions

The suspensions of commercial eucalyptus pulp showed greater stability compared to açai CNF ones (Figs. 4 and 5). *E-CNFs* presented final stability close to 95%, whereas the *A-CNFs* achieved 70% after 24 h. The exclusive addition of copaiba oil to eucalyptus CNFs (*Eco-CNFs*) did not cause significant changes in suspension stability for this raw material. The suspensions of açai CNFs with copaiba oil (*Aco-CNFs*) were slightly more stable compared to those of pure açai, reaching stability values of 85%. Functionalization of CNFs with both tannins and copaiba oil reduced the stability for both types of pulp since greater decantation was measured in the tubes. *ETco-CNF* suspensions achieved final stability close to 90%, indicating that additives caused little stability change after 24 h, whereas *ATco-CNFs* ones almost reached 65%.

The greater decantation of CNF suspensions from açai and eucalyptus with the addition of vegetal tannin occurred due to the high molecular weight of the tannin used. Tannins represent a class of polyphenolic macromolecules (500 –3000 Dalton) with relatively high polymerization degrees and a strong affinity for proteins and other biomolecules (Quideau et al. 2011). Due to the heightened ability to form complexes with other components, tannins are applied as coagulants/flocculants in the industry.

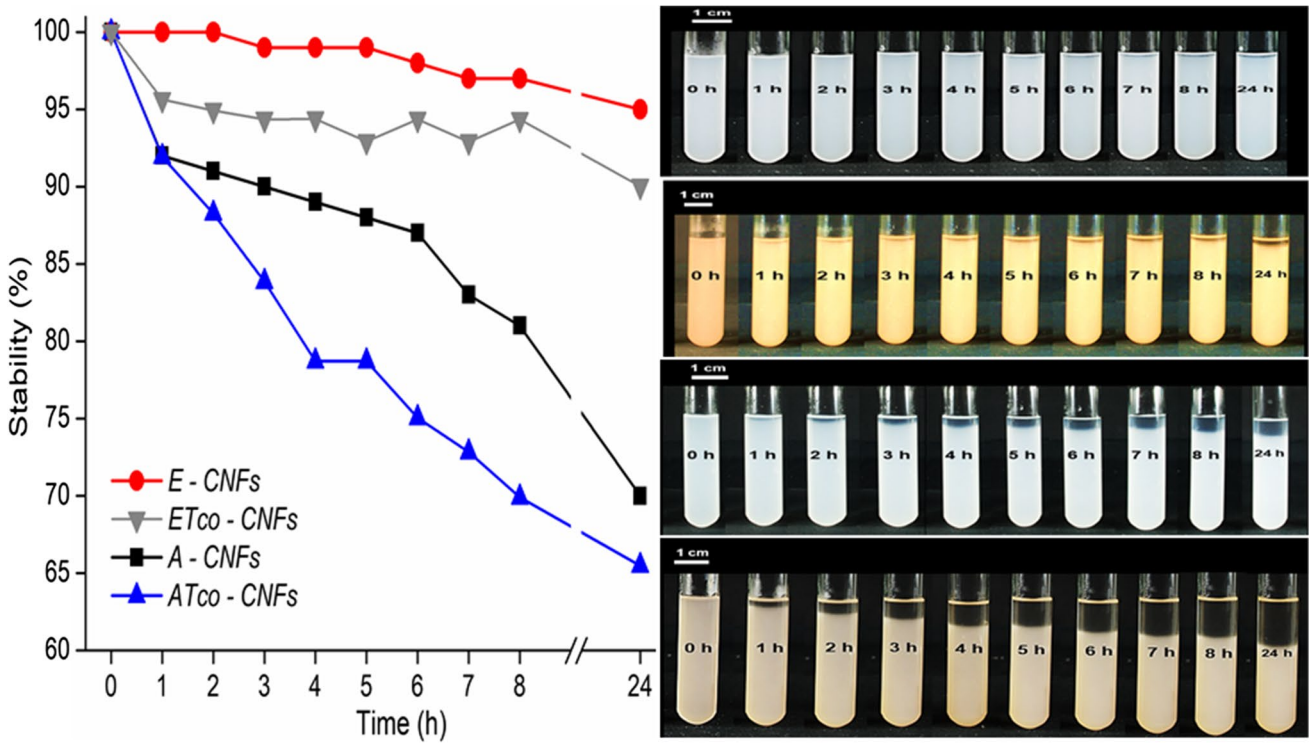

Fig. 4 Stability of the CNF suspensions produced: *E-CNFs*, *ETco-CNFs*, *A-CNFs*, *ATco-CNFs*.

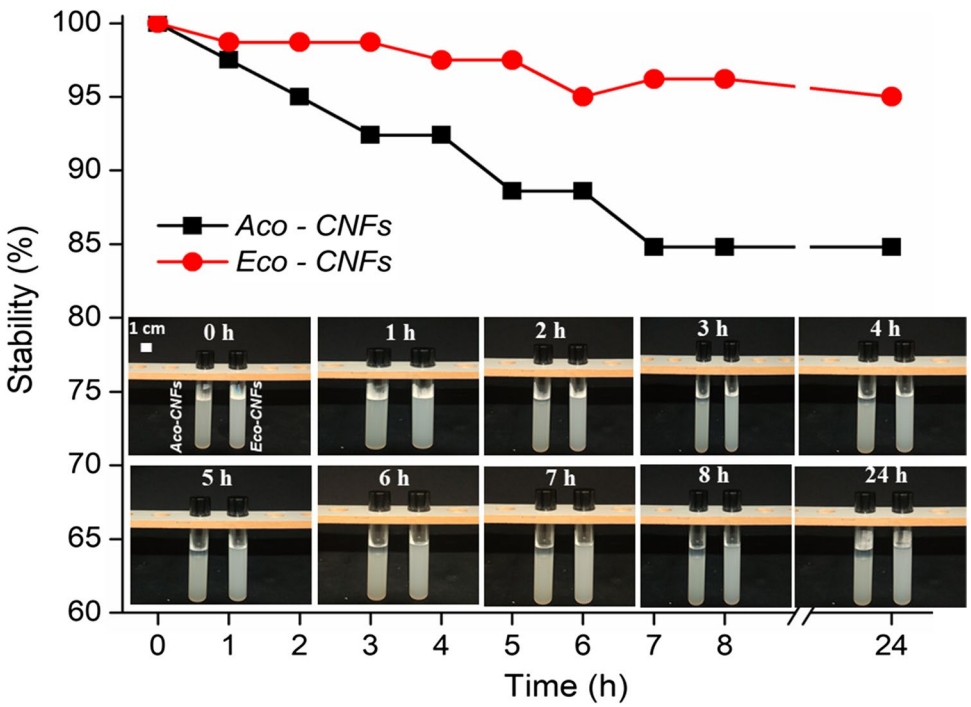

Fig. 5 Stability of the CNF suspensions produced: *Aco-CNFs* and *Eco-CNFs*.

Because of the correlation between particle size, aggregates, and stability, sedimentation analysis has been widely used to assess CNF quality (Butchosa and Zhou 2014). Nanoscale particles are kept in suspension by the Brownian motion, caused by interactions of repelling forces (Fukuzumi et al. 2014). Brownian motion is a random, uncontrolled movement of particles in a fluid as they constantly collide with others (Mitchell and Kogure 2006), which tends to

randomize fibrils orientation when the suspension is diluted enough to keep them dispersed.

SEM micrographs show the aspect of the CNF suspensions. Measurements of the structures' dimensions showed that the commercial eucalyptus pulp had a CNF average diameter lower than the açai fibers' one (Fig. 6). The eucalyptus pulp structures attained an average diameter of 64 nm, whereas those from açai fibers' pulp reached 251 nm. Therefore, CNFs from açai fibers can be considered a micro/nanoscale material since the minimum diameter found was 32 nm. Smaller or nanoscale dimensions allow a greater fibril intertwining due to the greater surface area, generating films with higher density and better physical and mechanical properties. Further, the açai fibrils with larger dimensions imply greater mass and more effective complexation with the tannins, increasing sedimentation.

Bulk density and water vapor permeability of the films

CNFs derived from açai pulp generated thicker films compared to eucalyptus pulp. Moreover, comparing the açai films among them, greater thicknesses were found for films with the additives copaiba oil and vegetal tannins. Among the eucalyptus films, no significant statistical differences were found when functionalized with copaiba oil and vegetal tannins. The bulk densities found for the açai and eucalyptus groups of films were statistically different by the Scott-Knott test ($\rho < 0.05$) (Table 3). Films produced with CNFs from commercial eucalyptus pulp obtained higher bulk density than the ones from açai fibers. Higher density film tends to provide better mechanical and barrier properties when compared to lower density one. The functionalization with copaiba oil and vegetal tannins did not significantly increase the bulk density of the two film groups. *ATco-CNF* films stood out among the evaluated treatments obtaining the highest grammage value. *ATco-CNF* suspensions, as previously mentioned, showed the lowest stability (see Figs. 4 and 5), indicating that the high mixture weight may have improved film's grammage. Films produced with eucalyptus CNFs were not statistically different among them in terms of grammage.

Table 3 Average thickness, bulk density, and grammage of the films produced.

Film	Thickness (μm)	Bulk density (g cm^{-3})	Grammage (g m^{-2})
A-CNFs	43 ± 12 b	0.820 ± 0.156*a	33.7 ± 1.9a
A_{CO}*-CNFs*	52 ± 6 c	0.902 ± 0.039a	36.8 ± 4.9a
AT_{CO}*-CNFs*	57 ± 8 c	0.917 ± 0.171a	51.6 ± 6.3b
E-CNFs	31 ± 1 a	1.163 ± 0.030b	35.5 ± 2.3a
E_{CO}*-CNFs*	33 ± 2 a	1.126 ± 0.104b	36.8 ± 2.1a
ET_{CO}*-CNFs*	34 ± 2 a	1.171 ± 0.037b	39.2 ± 2.4a

Averages followed by the same letter do not differ statistically by Scott-Knott test ($\rho < 0.05$); *standard deviation

The higher bulk density values for films produced with eucalyptus CNFs are reflected in their surface characteristics. Light microscopy images show that eucalyptus films had a more regular surface and fewer imperfections than the açai ones (Fig. 7). Copaiba oil was added in small content in relation to the dry mass of CNFs (5% wt) and therefore exerted little influence on the films' surface aspect. The tannin addition to the CNFs provided characteristic color seen in Fig. 7e, f, k, and l.

As seen before, the structures that form the eucalyptus films had a smaller average diameter than the açai CNFs (see Fig. 6). Smaller diametric structures concentrate greater

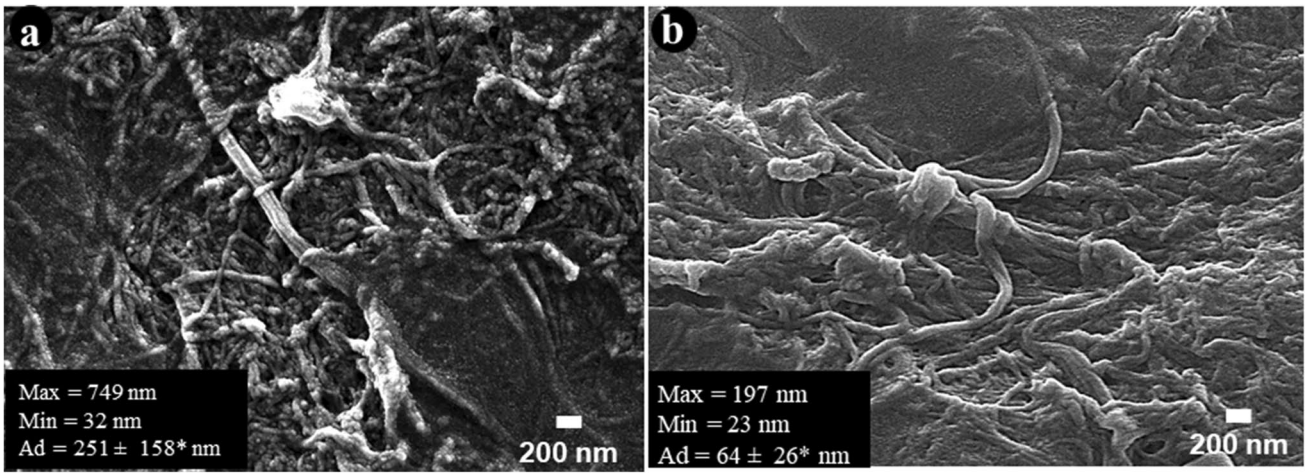

Fig. 6 Typical SEM images of the CNFs from **a** açai fibers and **b** eucalyptus; Max, maximum diameter; Min, minimum diameter; Ad, average diameter; *standard deviation.

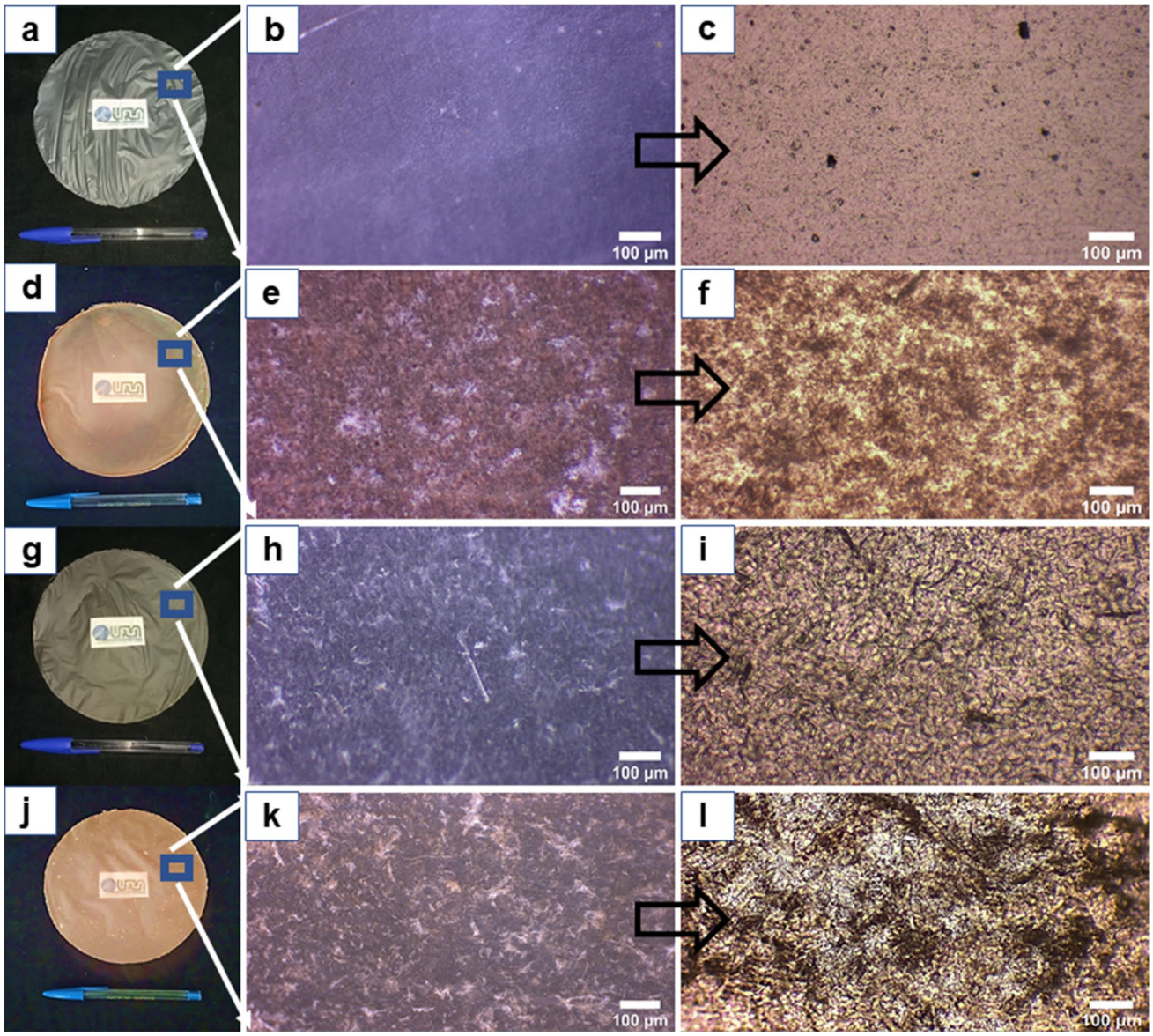

Fig. 7 Surface aspect of the CNF films produced: **a**, **b**, and **c** eucalyptus nanofibril films; **d**, **e**, and **f** eucalyptus nanofibril films with copaiba oil and vegetal tannin; **g**, **h**, and **i** açai nanofibril films; **j**, **k**, and **l** açai nanofibril films with copaiba oil and vegetal tannin. *__b__, __e__, __h__, and __k__ correspond to images obtained with a light source external to the microscope; __c__, __f__, __i__, and __l__ correspond to images obtained from the microscope internal light source, which passes through the sample.

surface area, promoting more efficient bindings and connections between fibrils. These connections improve compaction at film's surface and bulk. Fig. 7h and k shows gaps and empty spaces resulting from the lower efficient interlacing of açai CNFs. Despite the higher densities of eucalyptus CNF films and their forming structures of smaller dimensions, the *ATco-CNF* films obtained the lowest water vapor transmission rate (WVTR) (Fig. 8).

In the case of açai nanofibrils, functionalization with copaiba oil and vegetable tannins reduced vapor crossing through the film. According to Bonan et al. (2015), the copaiba oil shows a hydrophobic nature, which may have contributed to certain repulsion of water vapor. The hydrophobic structure of vegetal oils hinders their compatibility with fibers, requiring the use of a compatibilizer. The addition of oils from vegetal sources has already achieved positive results to reduce water vapor permeability in films for active packaging systems due to the formation of more apolar regions in their matrix (Brandelero et al. 2015). In addition, the açai fibers showed higher contents of non-cellulosic components, which may have hindered the vapor transfer through the film. Previous research has shown that lignin interaction between other biomolecules involves three major non-covalent bonds: hydrophobic, electrostatic, and

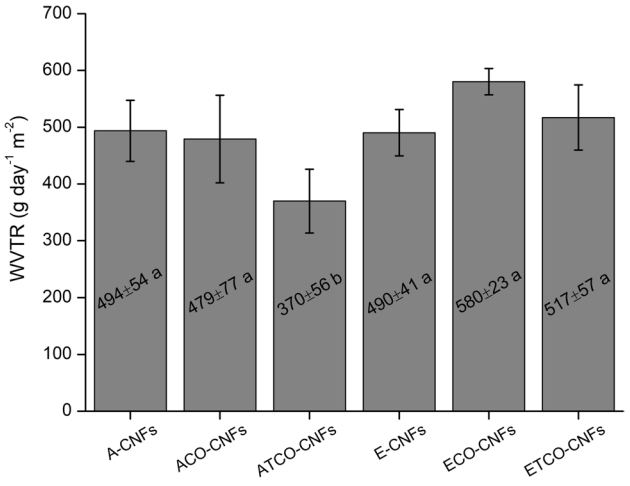

Fig. 8 Water vapor permeability of the films produced; averages followed by the same letter do not differ statistically by Scott-Knott test ($\rho < 0.05$).

hydrogen bonds (Guo and Wang 2014). Additionally, bonds between vegetal tannins and non-cellulosic molecules may have occurred due to tannins' complexing ability, reinforcing the hydrophobic character of the film.

The WVTR results were similar to those found in the literature regarding films produced with lignocellulosic wastes. The ideal structure of CNF networks is a compact complex form, presenting an obstacle to water vapor diffusion. Guimarães et al. (2021), studying films produced with CNFs from banana pseudostem wastes, found values of 519 and 497 g day^{-1} m^{-2} for WVTR after 20 and 40 passages through the fibrillator, respectively. Similarly, Stark (2016) developed films from bleached softwood CNFs and bleached hardwood CNFs and found WVTR of 686 and 606 g day^{-1} m^{-2}, respectively. These are potential results for packaging applications and advancement in pre-screening renewable raw materials to substitute petroleum-based polymers applied in multilayer packaging.

All produced films, functionalized or not with copaiba oil and vegetal tannins, achieved the maximum score (12) in the grease resistance test. The high surface resistance presented by nanostructured materials was generated by the efficient intertwining of cellulose fibrils, which prevents the penetration of grease substances.

Thermogravimetric analysis of the films

Thermogravimetric analysis shows that *ATco-CNF* films attained the highest temperature of maximum thermal degradation (T*max*) (Fig. 9; Table 4), whereas *A-CNFs* ones presented the lowest temperature of starting degradation (T*onset*). The interval between T*onset* and T*max* was 60 °C and 67 °C for *A-CNF* and *ATco-CNF* films, respectively. Açai fibers *in natura* presented a considerable amount of extractives (4%) and high content of hemicelluloses (26%) (see Table 2). Overall, some kinds of extractives thermally decompose at higher temperatures (250–550 °C) compared to hemicelluloses, improving thermal degradation resistance (Mészáros et al. 2007; Protásio et al. 2019). Therefore, for the açai CNFs, the addition of copaiba oil and vegetal tannin increased both T*onset* and T*max* temperatures. Regarding all the treatments involving eucalyptus CNFs, the additives did not cause significant interference in degradation temperatures.

The composition of copaiba oil may be one of the factors that increased the thermal degradation temperature of açai films. Copaiba oil consists of two classes of organic molecules, namely diterpenes (resin) and sesquiterpenes (essential oil) (Veiga Junior and Pinto 2002; Trindade et al. 2018). Santos (2019) evaluated the thermal degradation behavior of copaiba oil and found no changes in its molecular properties or mass loss up to approximately 97 °C. Between 97 and 212 °C, the mass of copaiba oil reduces to about 54%, probably due to the volatilization of essential oils, represented by sesquiterpene acid molecules. In the temperature range of 212–350 °C, the mass of the copaiba oil reduces to 0.26% as a consequence of the degradation of their resinous part, composed of diterpenoid acid molecules.

The compositions *ATco-CNFs* and *ETco-CNFs* also showed higher percentages of residues at the end of the thermogravimetric analysis. *ETco-CNF* film, specifically, presented 27% of residue. The commercial eucalyptus pulp presented a chemical composition with expressive purity, free of residual lignin. Generally, some phenolic substances, such as lignin, are chemical structures with high thermal stability (Protásio et al. 2020). Xie et al. (2021) studied different isocyanates with the addition of lignin and observed a thermal stability gain. Furthermore, Zhang et al. (2015) concluded that incorporation of lignin increased the T*max* of polyurethane composites, presumably assigned to extensive aromatic groups and benzene rings in lignin.

The more complex chemical composition of the açaí fibers' pulp, independent of the copaiba oil and vegetal tannins additions, promoted greater resistance to thermal degradation than compositions without other components. Such behavior was assumed to be a consequence of the varied chemical composition of non-cellulosic substances remaining after chemical treatments of açai fibers.

Mechanical properties of the films

Films produced with commercial pulp, with or without copaiba oil and vegetal tannin additives, were generally more resistant compared to açai ones. For both raw materials, tensile strength decreased with the addition of copaiba oil and vegetable tannins (Table 5). For the açai films, the

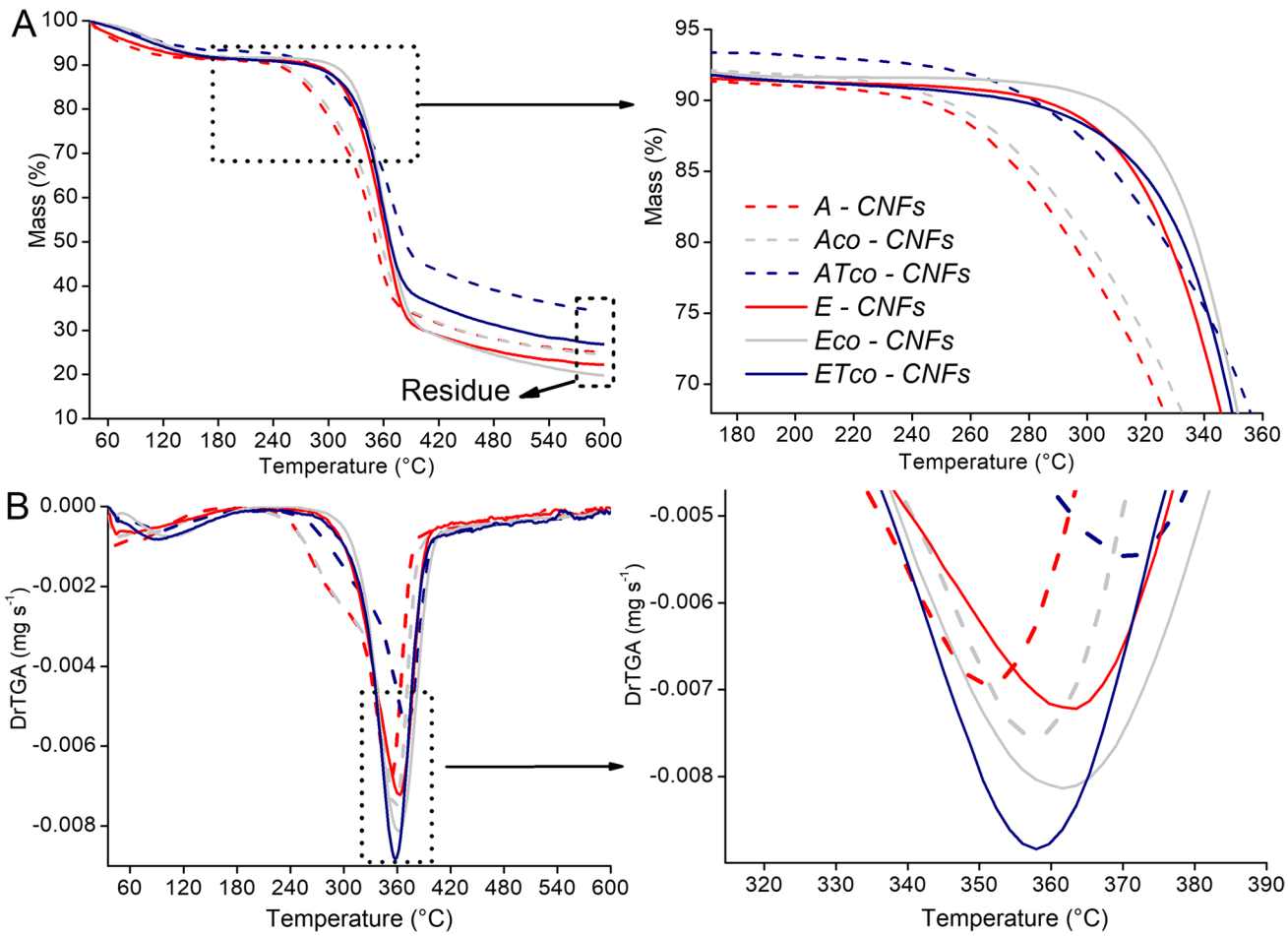

Fig. 9 Thermal degradation of the CNF films produced; **A** mass loss of with the increase of temperature; **B** first TGA derivative (DrTGA).

Table 4 Thermal behavior of the CNF films.

Film	T_{onset} °C	T_{max}	Residue (%)
A-CNFs	290	350	25
A_{CO}*-CNFs*	302	357	25
AT_{CO}*-CNFs*	303	370	33
E-CNFs	308	362	22
E_{CO}*-CNFs*	308	361	18
ET_{CO}*-CNFs*	312	358	27

Table 5 Mechanical properties of the films produced.

Film	Tensile strength (MPa)
A-CNFs	97.2 ± 4
A_{CO}*-CNFs*	35.9 ± 0.9
AT_{CO}*-CNFs*	31.3 ± 2
E-CNFs	133.8 ± 10
E_{CO}*-CNFs*	121.4 ± 3
ET_{CO}*-CNFs*	99.8 ± 9

Averages followed by the same letter do not differ statistically by Scott-Knott test ($\rho < 0.05$).

tensile strength reduced more than 63% with the addition of the copaiba oil and 68% when both components were used in the film's formulations. However, for films produced with commercial eucalyptus pulp, this reduction was less accentuated.

The addition of copaiba oil caused a 10% reduction in tensile strength of E_{CO}*-CNFs* films, whereas the use of both additives reduced it by 25%. Copaiba oil may result in a discontinuous matrix with larger porosity and cavities than those presented by the control films (Brandelero et al. 2015). Another factor to consider is that copaiba oil can disrupt the entanglement of CNFs. The stress-strain curves highlighted that *E-CNFs* and E_{CO}*-CNF* films were superior in mechanical strength among all the treatments (Fig. 10).

As previously mentioned, the addition of copaiba oil and vegetal tannins did not significantly increase the bulk density of açai and eucalyptus films (see Table 3). Guimarães

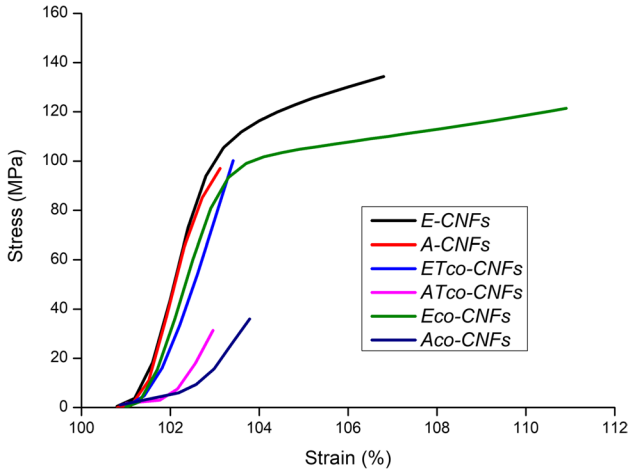

Fig. 10 Typical stress × strain curves of the films produced.

et al. (2021) produced films with banana pseudostem CNFs after 20 and 40 passages through the Supermasscolloider grinder that presented tensile strength of 46 and 51 MPa, respectively. These results were much lower than the values found in this research.

Colorimetric properties of the films

The total color difference (ΔE) and b values of the CNF films from açai and *eucalyptus* with the different additives were determined in the optical analysis (Fig. 11). Values obtained from *eucalyptus* films were similar comparing ET_{CO}*-CNFs*, E_{CO}*-CNFs*, and *E-CNFs*. *Eucalyptus* films with addition of copaiba oil (*Eco-CNFs*) presented slightly superior compared to the other treatments. For açai films, ΔE was slightly superior for AT_{CO}*-CNFs* and lower for A_{CO}*-CNFs*. Intermediate values were found for *A-CNFs* samples. In general, it can be stated that the incorporation of copaiba oil and vegetal tannin additives resulted in a greater disparity of values for the açai film than for *eucalyptus* films. ΔE indicates the degree of total color difference from the standard color plate (Ghanbarzadeh et al. 2010). In general, film color is influenced by factors such as the cross-linkage degree, treatment of the fibers, and fabrication process (Su et al. 2012). In the present work, all these factors may have greatly affected the color index of the films in relation to the raw material nature. The dimensions of the eucalyptus CNFs obtained smaller dimensions in relation to those generated from açai, as well as the eucalyptus films presented greater bulk density in relation to the açai films (see Table 3 and Fig. 6). Differences in density and, consequently, in levels of CNF aggregation may have caused different readings of the colorimetric parameters of the samples.

Contrary to the values of ΔE, parameter b was higher, in general, for films produced with açai CNFs and additives. Increases in b values are related to both yellowish and higher opacity of the films with the addition of copaiba oil and vegetal tannin, which can be noted without specific equipment. Although all the films exhibited apparently smooth surfaces at naked eye, a more detailed visualization at light microscopy reveals grainy surfaces (see Fig. 7). The pure films of açaí CNFs showed more darkened color due to the high content of lignin in their composition (see Table 2). As lignin is a natural binder, its presence may be related to the formation of grains during the drying procedure. This effect can be attributed to the coalescence of the structures formed during film drying, resulting in surface roughness (Ghanbarzadeh and Almasi 2011). In addition, the vegetal tannins also have a content of solid substances that may contribute to the formation of grains and accentuate the color of the films. This effect may have increased the b values of the films, especially in those produced from açai CNFs. The ideal appearance for films obtained from natural fibers should be as close to colorless as possible to simulate the colorimetric aspect of common polymeric films. Moreover, colored films may have the yellowish and darkened coloration enhanced with the time. Potential applications for films produced from CNFs include printing papers and packaging, for which high brightness cellulose pulp is desired; hence, *E-CNFs* and *Eco-CNFs* showed better possibilities for the final purpose. However, the color factor does not necessarily prevent the application of films for packaging and coatings.

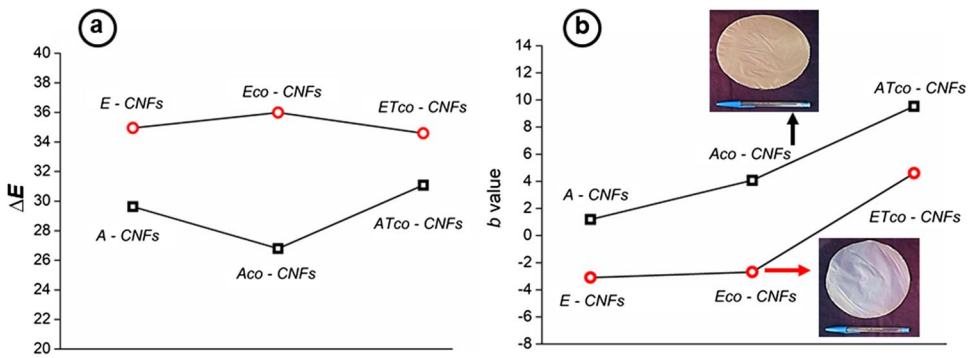

Fig. 11 Colorimetric properties of the CNF films produced: **a** total color difference (ΔE) of the CNF films; **b** b values of the films.

Acai fibers call for changes in the previous chemical treatments used here in order to enable more effective isolation of cellulose and improvement of the optical quality of the films.

Conclusion

In this study, CNF suspensions of açai and commercial eucalyptus pulp were functionalized with copaiba oil and vegetal tannins to produce films with possible packaging potential. The açai fibers presented a great resistance regarding the removal of non-cellulosic fiber components. Films of açai CNFs with tannin and copaiba oil addition attained the lowest water vapor transmission rate (WVTR) among all the treatments, 370 g day^{-1} m^{-2}. *ATco-CNF* films obtained the highest temperature of maximum thermal degradation (T*max*). The compositions *ATco-CNFs* and *ETco-CNFs* also showed higher percentages of residues after exposure to a temperature of 600 °C at the end of the thermogravimetric analysis. The addition of copaiba oil and vegetal tannins reduced mechanical strength properties for both CNFs films. The stress-strain curves highlighted that *E-CNFs* and E_{CO}*-CNFs* films were superior in mechanical strength and in other properties, in general, among all the treatments. The evaluation of colorimetry showed a greater tendency to yellowing for açai films, especially those functionalized with vegetal tannins. The films produced in this work, from the studied raw materials, functionalized with the proposed additives, and presented packaging potential regarding light and low-moisture products due to their suitable thermal and barrier characteristics. More studies should be carried out on pre-treatment of waste fibers in order to reduce energy consumption and improve their mechanical properties.

Acknowledgements The authors thank the Coordenacão de Aperfeiçoamento de Pessoa de Nível Superior (CAPES, Brazil), Conselho Nacional de Desenvolvimento Científico e Tecnológico (CNPq, finance code 300985/2022-3) for their financial support. Thanks also to the Brazilian Lignocellulosic Composites and Nanocomposites Network (RELIGAR), to the Biomaterials Engineering Graduation Program (PPGBIOMAT-UFLA, Brazil), and to State University of Amapa (UEAP) and Foundation for Research Support of Amapa (FAPEAP) (finance code 0022.0279.1202.0016/2021 - Edital 003/2021 postdoc scholarship). Finally, thanks go to the Laboratory of Electron Microscopy and Analysis of the Ultrastructural Federal University of Lavras, (http://www.prp.ufla.br/labs/microscopiaeletronica/) for the technical support for experiments involving electron microscopy.

Author contribution MVS contributed with the writing of the initial version, review, data collection, and data analysis. LB and MCD were major contributors in writing the manuscript, specifically writing the initial version, review, and editing of the manuscript. MSS and LMM contributed to the search for new raw materials resources and review. TMS, GHDT, and FTAJ contributed with supervision, conceptualization, funding acquisition, and project administration. All authors read and approved the final manuscript.

Funding Foundation for Research Support of Minas Gerais (FAPEMIG). Conselho Nacional de Desenvolvimento Científico e Tecnológico (CNPq, finance code 300985/2022-3). State University of Amapa (UEAP) and Foundation for Research Support of Amapa (FAPEAP) (finance code 0022.0279.1202.0016/2021 - Edital 003/2021 postdoc scholarship).

Data availability The datasets supporting the conclusions of this article are included in the article. Besides, the datasets used and/or analyzed during the current study are available from the corresponding author on reasonable request.

Declarations

Ethics approval and consent to participate Not applicable

Consent for publication Not applicable

Competing interests The authors declare no competing interests.

References

ABNT (2003) Brazilian Association of Technical Standards NBR 11941: Madeira – determination of basic density. Rio de Janeiro. 6p

Abraham E, Deepa B, Pothan LA, Jacob M, Thomas S, Cvelbar U, Anandjiwala R (2011) Extraction of nanocellulose fibrils from lignocellulosic fibres: a novel approach. Carbohydr Polym 86:1468–1475. https://doi.org/10.1016/j.carbpol.2011.06.034

Agrawal R, Saxena NS, Sharma KB, Thomas S, Sreekala MS (2000) Activation energy and crystallization kinetics of untreated and treat oil palm fibre reinforced phenol formaldehyde composites. Mater Sci Eng 277:77–82. https://doi.org/10.1016/S0921-5093(99)00556-0

Amaral AC, Bocca AL, Ribeiro AM, Nunes J, Peixoto DLG, Simioni AR, Primo FL, Lacava ZGM, Bentes R, Titze-de-Almeida R, Tedesco AC, Morais PC, Felipe MSS (2009) Amphotericin B in poly (lactic-co-glycolic acid) (PLGA) and dimercaptosuccinic acid (DMSA) nanoparticles against paracoccidioidomycosis. J Antimicrob Chemother 63:526–533. https://doi.org/10.1093/jac/dkn539

ASTM (2000) American Society for Testing and Materials - ASTM E 96-00. Standard test methods for water vapor transmission of materials, Philadelphia

ASTM (2018) American Society for Testing and Materials - ASTM D882. Standard test methods for tensile properties of thin plastic sheeting, West Conshohocken

Bian H, Gao Y, Yang Y, Fang G, Dai H (2018) Improving cellulose nanofibrillation of waste wheat straw using the combined methods of prewashing, p-toluenesulfonic acid hydrolysis, disk grinding, and endoglucanase post-treatment. Bioresour Technol 256:321–327

Bonan RF, Bonan PR, Batista AU, Sampaio FC, Albuquerque AJ, Moraes MC, Mattoso LH, Glenn GM, Medeiros ES, Oliveira JE (2015) In vitro antimicrobial activity of solution blow spun poly (lactic acid)/polyvinylpyrrolidone nanofibers loaded with Copaiba (Copaifera sp.) oil. Mater Sci Eng C Mater Biol Appl 48:372–377. https://doi.org/10.1016/j.msec.2014.12.021

Brandelero RPH, Almeida FM, Alfaro A (2015) Microestrutura e propriedades de filmes de amido-álcool polivinílico-alginato adicionados de óleos essenciais de copaíba e capim limão. Química Nova 38:910–916. https://doi.org/10.5935/0100-4042.20150098

Browning BL (1963) The chemistry of wood. Interscience, Warrenvile, p 689

Bufalino L, de Sena Neto AR, Tonoli GHD, de Souza Fonseca A, Costa TG, Marconcini JM, Colodette JL, Labory CRG, Mendes LM (2015) How the chemical nature of Brazilian hardwoods affects nanofibrillation of cellulose fibers and film optical quality. Cellulose 22:3657–3672. https://doi.org/10.1007/s10570-015-0771-3

Butchosa N, Zhou Q (2014) Water redispersible cellulose nanofibrils adsorbed with carboxymethyl cellulose. *Cellulose 21*:4349–4358. https://doi.org/10.1007/s10570-014-0452-7

Cano A, Contreras C, Chiralt A, González-Martínez C (2021) Using tannins as active compounds to develop antioxidant and antimicrobial chitosan and cellulose based films. Carbohydr Polymer Technol Appl 2:100156. https://doi.org/10.1016/j.carpta.2021.100156

Chen W, Abe K, Uetani K, Yu H, Liu Y, Yano H (2014) Individual cotton cellulose nanofibrils: pretreatment and fibrillation technique. Cellulose 21:1517–1528. https://doi.org/10.1007/s10570-014-0172-z

Coutts RSP, Warden PG (1992) Sisal pulp reinforced cement mortar. Cem Concr Compos 14:17–21. https://doi.org/10.1016/0958-9465(92)90035-T

Debone HS, Lopes PS, Severino P, Yoshida CMP, Souto EB, da Silva CF (2019) Chitosan/Copaiba oleoresin films for would dressing application. Int J Pharm 555:146–152. https://doi.org/10.1016/j.ijpharm.2018.11.054

Dias M, Mendonça M, Damásio R, Zidanes U, Mori F, Ferreira S, Tonoli G (2019) Influence of hemicellulose content of eucalyptus and pinus fibers on the grinding process for obtaining cellulose micro/nanofibrils. Holzforschung 73:1035–1046. https://doi.org/10.1515/hf-2018-0230

do Lago RC, de Oliveira ALM, Dias MC, de Carvalho EEN, Tonoli GHD, Vilas Boas EVB (2020) Obtaining cellulosic nanofibrils from oat straw for biocomposite reinforcement: mechanical and barrier properties. Ind Crop Prod 148:112264. https://doi.org/10.1016/j.indcrop.2020.112264

Fonseca CS, Scatolino MV, Silva LE, Martins MA, Guimarães M Jr, Tonoli GHD (2021) Valorization of jute biomass: performance of fiber–cement composites extruded with hybrid reinforcement (fibers and nanofibrils). Waste Biomass Valor. https://doi.org/10.1007/s12649-021-01394-1

Fukuzumi H, Tanaka R, Saito T et al (2014) Dispersion stability and aggregation behavior of TEMPO-oxidized cellulose nanofibrils in water as a function of salt addition. Cellulose 21:1553–1559. https://doi.org/10.1007/s10570-014-0180-z

Furtado PS, Melo JRS, Meireles PW, Honorio TS, Miguel NCO et al (2021) Benign prostatic hyperplasia therapy through liquisolid technology composed of polymer-layered nanocomposites based on silicate that contain babassu oil and copaiba oil-resin. J Drug Deliv Sci Technol. https://doi.org/10.1016/j.jddst.2021.102586

Ghanbarzadeh B, Almasi H (2011) Physical properties of edible emulsified films based on carboxymethyl cellulose and oleic acid. Int J Biol Macromol 48:44–49. https://doi.org/10.1016/j.ijbiomac.2010.09.014

Ghanbarzadeh B, Almasi H, Entezami AA (2010) Physical properties of edible modified starch/carboxymethyl cellulosefilms. Innov Food Sci 11:697–702. https://doi.org/10.1016/j.ifset.2010.06.001

Guimarães M Jr, Botaro VR, Novack KM, Teixeira FG, Tonoli GHD (2015) Starch/PVA-based nanocomposites reinforced with bamboo nanofibrils. Ind Crop Prod 70:72–83. https://doi.org/10.1016/j.indcrop.2015.03.014

Guimarães M Jr, Teixeira FG, Tonoli GHD (2018) Effect of the nanofibrillation of bamboo pulp on the thermal, structural, mechanical and physical properties of nanocomposites based on starch/poly (vinyl alcohol) blend. Cellulose. 25:1–27. https://doi.org/10.1007/s10570-018-1691-9

Guimarães BMR, Scatolino MV, Martins MA et al (2021) Bio-based films/nanopapers from lignocellulosic wastes for production of added-value micro-/nanomaterials. Environ Sci Pollut Res. https://doi.org/10.1007/s11356-021-16203-4

Guo F, Wang R (2014) On the persistence and unique continuation properties for an integrable two-component Dullin–Gottwald–Holm system. Nonlinear Anal: Theory Methods Appl 96:38–46. https://doi.org/10.1016/j.na.2013.10.021

Kennedy F, Phillips GO, Williams EPA (1987) Wood and cellulosic: industrial utilization, biotechnology, structure and properties. Halsted, New York, p 1130

Leiviskä T, Rämö J (2008) Coagulation of wood extractives in chemical pulp bleaching filtrate by cationic polyelectrolytes. J Hazard Mater 153:525–531. https://doi.org/10.1016/j.jhazmat.2007.08.084

Leiviskä T, Rämö J, Nurmesniemic H, Pöykiö R, Kuokkanene T (2009) Size fractionation of wood extractives, lignin and trace elements in pulp and paper mill wastewater before and after biological treatment. Water Res 43:3199–3206. https://doi.org/10.1016/j.watres.2009.04.051

Linan LZ, Cidreira ACM, Rocha CQ, Menezes FF, Rocha GJM, Paiva AEM (2021) Utilization of acai berry residual biomass for extraction of lignocellulosic byproducts. J Bioresources Bioprod. https://doi.org/10.1016/j.jobab.2021.04.007

Mészáros E, Jakab E, Várhegyi G (2007) TG/MS, Py-GC/MS and THM-GC/MS study of the composition and thermal behavior of extractive components of *Robinia pseudoacacia*. J Anal Appl Pyrolysis 79:61–70. https://doi.org/10.1016/j.jaap.2006.12.007

Missio André L, Mattos BD, Ferreira DF, Magalhães WLE, Bertuol DA, Gatto DA, Petutschnigg A, Tondi G (2018) Nanocellulose-tannin films: from trees to sustainable active packaging. J Clean Prod 184:143–151. https://doi.org/10.1016/j.jclepro.2018.02.205

Mitchell JG, Kogure K (2006) Bacterial motility: links to the environment and a driving force for microbial physics. FEMS Microbiol Ecol 55:3–16. https://doi.org/10.1111/j.1574-6941.2005.00003.x

Morelli CL, Mahrous M, Belgacem MN, Branciforti MC, Bretas RES, Bras J (2015) Natural copaiba oil as antibacterial agent for biobased active packaging. Ind Crop Prod 70:134–141. https://doi.org/10.1016/j.indcrop.2015.03.036

Okahisa Y, Furukawa Y, Ishimoto K, Narita C, Intharapichai K, Ohara H (2018) Comparison of cellulose nanofiber properties produced from different parts of the oil palm tree. Carbohydr Polym 198:313–319. https://doi.org/10.1016/j.carbpol.2018.06.089

Paschoalick TM, Garcia FT, Sobral PJA, Habitante AMQB (2003) Characterization of some functional properties of edible films based on muscle proteins of Nile tilapia. Food Hydrocoll 17:419–427. https://doi.org/10.1016/S0268-005X(03)00031-6

Pena DWP, Tonoli GHD, de Paula PT et al (2021) Exfoliating agents for skincare soaps obtained from the crabwood waste bagasse, a natural abrasive from Amazonia. Waste Biomass Valor 12:4441–4461. https://doi.org/10.1007/s12649-020-01336-3

Pizzi A (2008) Tannins: major sources, properties and applications. In: Belgacem MN, Gandini A (eds) Monomers, polymers and composites from renewable resources. Elsevier, Amsterdam, p 553

Protásio TP, Scatolino MV, Araújo ACC, Oliveira AFCF, Figueiredo ICR, Assis MR, Trugilho PF (2019) Assessing proximate composition, extractive concentration, and lignin quality to determine appropriate parameters for selection of superior *Eucalyptus* firewood. BioEnergy Res 12:626–641. https://doi.org/10.1007/s12155-019-10004-x

Protásio TP, Scatolino MV, Lima MDR, Araújo ACC, Figueiredo ICR, Bufalino L, Hein PRG, Trugilho PF (2020) Insights in quantitative indexes for better grouping and classification of eucalyptus clones

used in combustion and energy cogeneration processes in Brazil. Biomass Bioenergy 143:105835. https://doi.org/10.1016/j.biombioe.2020.105835

Quideau S, Deffieux D, Douat-Casassus C, Pouységu L (2011) Plant polyphenols: chemical properties, biological activities and synthesis. Angew Chem Int Ed 50:586–621. https://doi.org/10.1002/anie.201000044

Santana JS, do Rosário JM, Pola CC, Otoni CG, Soares NFF, Camilloto GP, Cruz RS (2017) Cassava starch-based nanocomposites reinforced with cellulose nanofibrils extracted from sisal. J Appl Polym Sci 134:44637. https://doi.org/10.1002/app.44637

Santos JG (2019) The thermodynamic method of vitrification of copaíba oil-resin (*Copaifera Langsdorffii*). Int J of Sci Res, 8. https://www.ijsr.net/archive/v8i2/ART20194751. Accessed on 14 May 2021

Scandinavian Pulp, Paper and Board Testing Committee (2000) Method SCAN-C 62:00, Water retention value of chemical pulps.

Scatolino MV, Bufalino L, Mendes LM, Guimarães Júnior M, Tonoli GHD (2017) Impact of nanofibrillation degree of eucalyptus and Amazonian hardwood sawdust on physical properties of cellulose nanofibril films. Wood Sci Technol 51:1095–1115. https://doi.org/10.1007/s00226-017-0927-4

Scatolino MV, Fonseca CS, da Silva GM et al (2018) How the surface wettability and modulus of elasticity of the Amazonian paricá nanofibrils films are affected by the chemical changes of the natural fibers. Eur J Wood Prod 76:1581–1594. https://doi.org/10.1007/s00107-018-1343-7

Schindelin J, Arganda-Carreras I, Frise E, Kaynig V, Longair M, Pietzsch T, Preibisch S, Rueden C, Saalfeld S, Schmid B, Tinevez JY, White DJ, Hartenstein V, Eliceiri K, Tomancak P, Cardona A (2012) Fiji: an open-source platform for biological-image analysis. Nature methods 9:676–682. https://doi.org/10.1038/nmeth.2019

Souza LO, Lessa OA, Dias MC, Tonoli GHD, Rezende DVB, Martins MA, Neves ICO, de Resende JV, Carvalho EEN, Vilas Boas EVB, de Oliveira JR, Franco M (2019) Study of morphological properties and rheological parameters of cellulose nanofibrils of cocoa shell (*Theobroma cacao* L.). Carbohydr Polym 214:152–158. https://doi.org/10.1016/j.carbpol.2019.03.037

Stark NM (2016) Opportunities for cellulose nanomaterials in packaging films: a review and future trends. J Renew Mater 4:313–326. https://doi.org/10.7569/JRM.2016.634115

Su J, Yuan X, Huang Z, Wang X, Lu X, Zhang L, Wang S (2012) Physicochemical properties of soy protein isolate/carboxymethyl cellulose blend films crosslinked by Maillard reactions: color, transparency and heat-sealing ability. Mater Sci Eng C 32:40–46. https://doi.org/10.1016/j.msec.2011.09.009

TAPPI (2002) Technical Association of the Pulp and Paper Industry T 222 om-02, Acid insoluble lignin in wood and pulp

TAPPI (2012a) Technical Association of the Pulp and Paper Industry T 211 om-12, Ash in wood, pulp, paper, and paperboard: combustion at 525°C.

TAPPI (2012b) Technical Association of the Pulp and Paper Industry T 559 cm-12, Grease resistance test for paper and paperboard.

TAPPI (2017) Technical Association of the Pulp and Paper Industry T 204 cm-17, Solvent extractives of wood and pulp.

Trindade R, da Silva JK, Setzer WN (2018) Copaifera of the neotropics: a review of the phytochemistry and pharmacology. Int J Mol Sci 19:1511. https://doi.org/10.3390/ijms19051511

Veiga Junior VF, Pinto AC (2002) The *Copaifera L.* genus. Quim Nova 25:273–286. https://doi.org/10.1590/S0100-40422002000200016

Xie H, Zhang H, Liu X, Tian S, Liu Y, Fu S (2021) Ag immobilized lignin-based PU coating: a promising candidate to promote the mechanical properties, thermal stability, and antibacterial property of paper packaging. Int J Biol Macromol 189:690–697. https://doi.org/10.1016/j.ijbiomac.2021.08.184

Yue Y, Han J, Han G, Zhang Q, French AD, Wu Q (2015) Characterization of cellulose I/II hybrid fibers isolated from energycane bagasse during the delignification process: morphology, crystallinity and percentage estimation. Carbohydr Polym 133:438–447. https://doi.org/10.1016/j.carbpol.2015.07.058

Zhang C, Wu H, Kessler MR (2015) High bio-content polyurethane composites with urethane modified lignin as filler. Polymer 69:52–57. https://doi.org/10.1016/j.polymer.2015.05.046

Zhang C, Nair SS, Chen H, Yan N, Farnood R, Li F (2019) Thermally stable, enhanced water barrier, high strength starch biocomposite reinforced with lignin containing cellulose nanofibrils. Carbohydr Polym 230:115626. https://doi.org/10.1016/j.carbpol.2019.115626

Zhou Y, Zhou X, Li B, Xu Y, Essawy H, Wu Z, Du G (2019) Tannin-furanic resin foam reinforced with cellulose nanofibers (CNF). Ind Crop Prod 134:107–112